RSC Advances

ROYAL SOCIETY OF CHEMISTRY

www.rsc.org/advances

Cite this: DOI: 10.1039/c0xx00000x

www.rsc.org/xxxxxx

Paper

Dispersion of muti-walled carbon nanotubes modified by rosemary acid into poly (vinyl alcohol) and preparation of their composite fibers

Pei Zhang, Tengfei Zhou, Liucheng He, Shiyu Zhang, Jun Sun, Jianjun Wang, Chuanxiang Qin, Lixing Dai*

Received (in XXX, XXX) Xth XXXXXXXXX 20XX, Accepted Xth XXXXXXXXX 20XX
DOI: 10.1039/b000000x

PVA was reinforced with MWCNTs using rosemary acid as a dispersant for the first time to achieve good dispersity of the MWCNTs in PVA matrix and finally high-performance composite fibers. The MWCNTs/rosemary acid (m-MWCNTs) system was uniformly dispersed in water/DMSO mixed solvent, and then m-MWCNTs were dispersed in PVA solutions in the same solvent to form spinning dope, from which PVA/m-MWCNTs composite fibers were prepared by gel-spinning followed by a hot-drawing process. The results showed that the obtained fibers possessed high tensile strengths up to 600 MPa and Young's moduli to about 35 GPa, much higher than those of pure PVA fiber. Raman, ^{1}H NMR and TEM were used to probe the structural characteristics and the dispersion properties of m-MWCNT.

1. Introduction

As a one-dimensional material, carbon nanotubes (CNTs) are considered to be ideal fillers for fibers since they possess unique electrical, thermal, and mechanical properties, especially high tensile strength and modulus [1-3]. CNTs reinforced composites have gained their popularity to researchers over the past decade because of their excellent physical and chemical performance and potential applications [4, 5]. Plenty of studies about CNTs reinforced nanocomposites have indicated that CNTs are effective to enhance the mechanical properties of polymer matrices, but their poor dispersion and the low interaction with the matrix polymer are the main problems which hindered the reinforcement characteristics [6].

CNTs have an inherent tendency to aggregate and become entangled to form networks because of their bundle-like structures with a high number of van der Waals interactions [7], causing extremely poor solubility in water or organic solvents, which limited the practical use of the composite materials. Therefore considerable research efforts have already been devoted to develop processes for their effective dispersion, and there commonly are two main routes for the separation of CNTs, covalent attachment of chemical groups, through reactions on the conjugated skeleton of CNTs [8], and non-covalent adsorption or wrapping of various functional molecules onto the tubes [9].

The most popular method of covalent modification first reported by Liu *et al.*[10] is treating CNTs in acid to bring oxidized groups to their surface, carboxyl groups will generate negatively charged ions after hydrolysis, and strong electrostatic repulsions between the carboxylated CNTs forces them to disperse uniformly in the solution, which helps them to intimately mix with the polymer matrix [11]. At the same time, carboxylated CNTs were extensively used as precursors for further covalent modification of CNTs, through esterification [12], amidation [13], or complexation [14] reactions. However, acidification can induce a large amount of defects, restricting the strength enhancement of the CNT composites. There are also other covalent modifications for CNTs such as cycloaddition reactions [15, 16], radical [17-19], nucleophilic [20] and electrophilic additions [21], while all the reaction conditions are too harsh and the processes are considerably complicated to achieve commercial feasibility.

Noncovalent modification is now adding its appeal for many researchers since it does not damage the conjugated structure of CNT sidewalls and is more feasible than covalent modification [22]. The dispersion of noncovalent modification is achieved by interaction of secondary van der vaals bonding or hydrogen-bonding between a dispersant and CNT surface. O'Connell *et al.*[23] reported that single-wall carbon nanotubes (SWCNTs) have been suspended in aqueous media as individuals surrounded by a sodium dodecyl sulfate (SDS) adsorbed phase. Islam et al.[24] used sodium dodecylbenzene sulfonate (SDBS) to solubilize high weight fraction SWCNTs in water by the nonspecific physical adsorption. Elizabeth *et al.* [25] found dodecyl trimethylammonium bromide (DTAB) to form exceptionally stable SWCNT dispersions.

Recently, natural molecules with a hydrophilic surface have been used in composites with CNTs by physical interaction. Because of natural affinity for protein in aqueous ferritin solution, SWCNTs were functionalized with ferritin, resulting in significant ferritin-SWCNTs conjugation and the solubilization of SWCNTs [26]. Liu *et al.*[27] described a non-destroyable surface decoration of CNTs with biopolymer chitsoan via a controlled surface-deposition and cross linking process. Particularly, green tea and its extractive have attracted considerable amount of attention due to their green, healthy characteristics and good functionalization effect. Nakamura *et al.*[28] discovered that a green

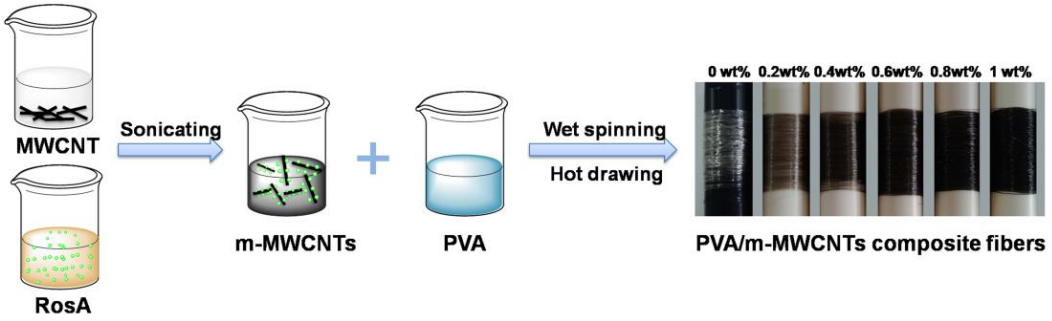

Fig. 1 Schematic illustration of the preparation process of PVA/m-MWCNTs composite fibers.

tea solution can dissolve SWCNTs without aggregation as an aqueous medium. In our previous study [29], strength and modulus of poly (vinyl alcohol) (PVA) fibers were extremely increased by introduction of MWCNTs functionalized with tea polyphenols. It was reported that π-π stacking between the benzene ring of surfactant and MWCNTs was the major factor that account for the CNTs dispersion.

Rosemary acid (RosA) having similar structure to polyphenols is an extract from rosemary, which is an evergreen shrub, with lovely aromatic linear leaves. So, as a natural phenolic compound, RosA is green, non-toxic and environment-friendly. Like tea polyphenols, it possesses benzene rings and hydroxyl groups in the structure, which are a base of π–π stacking interaction between RosA and CNTs and interaction between RosA functionalized CNTs and polymer matrix in CNTs filled polymer composites, respectively. Besides, there are an ester group, a carboxyl group and isolated double bond between two benzene rings in the linear structure of RosA, which gives the molecule better flexibility, causing a superior performance in dispersing MWCNTS in polymer matrix. In addition, compared with polyphenols, its more hydroxyl groups and added carboxyl group have more chances to interact with polymer in which it can disperse better.

Poly(vinyl alcohol) (PVA) has been considered as a suitable matrix for CNTs composites, since it has a large number of hydroxyl in the main chain which enables the polymer to form hydrogen bonds with RosA easily. In the current work, we attempted to disperse MWCNTs in PVA solution with the assistance of RosA to obtain PVA composite fibers with high strength and modulus. MWCNTs modified by RosA (m-MWCNTs) and PVA dissolved in DMSO/H_2O mixed solvent, then the uniform mixture was spun by wet spinning process, and finally the as-spun fiber was drawn. The structure and properties of the PVA/m-MWCNTs composite fibers containing different RosA content were investigated. Results showed that the strength and modulus of the composite fibers were surprisingly increased, and the strengthening mechanism of MWCNTs in the composite fibers was proposed.

2. Experimental procedure

2.1 Materials

PVA (degree of polymerization 1750, alcoholysis degree 98%, M_w=74800) and Dimethyl sulfoxide (DMSO) were bought from Sinopharm Chemical Reagent Co., Ltd (China). MWCNTs (outer diameter 20-30nm and length 10-30μm) were purchased from Chengdu Organic Chemicals Co., Ltd. (China). RosA (purity>97%) was purchased from Aladdin Chemistry Co., Ltd (China).

2.2 Modification of MWCNTs in RosA solution

0.1, 0.3, 0.5, 0.7 and 0.9 wt% RosA solutions were prepared respectively in DMSO/H_2O (vol ratio=3/1) at room temperature. 0.06wt% MWCNTs were then added and sonicated for 2 h using an ultrasonic instrument (40 kHz, 70 W) produced by Kunshan Ultrasonic Instrument Co., Ltd., China. The resulting m-MWCNTs dispersions in the DMSO/H_2O mixed solvent were separated into two groups for characterization and for mixing with PVA. As a contrast, the MWCNTs without RosA (p-MWCNTs) were also sonicated for 2 h.

2.3 Preparation of PVA/m-MWCNTs composite fibers

PVA pellets were dissolved in DMSO/H_2O (vol ratio=3/1) by heating at 90 ^oC with stirring to prepare 17 wt% solutions. The above prepared m-MWCNTs dispersions were poured into the PVA solution and stirred at 90^oC for 1 h to form new mixture, and the final PVA concentration was adjusted to 14 wt%. Composite fibers were prepared by wet spinning and drawing at a ratio of 12 as described in our previously work [30]. A set of the composite fibers with m-MWCNTs mass fractions of 0, 0.2, 0.4, 0.6, 0.8 and 1 wt% were obtained as shown in Fig. 1.

2.4 Characterization

UV transmission spectra of m-MWCNTs dispersions were measured via a Varian CARY50 Ultraviolet-visible (UV-vis) spectrometer. ^{1}H-NMR spectra were recorded in D_2O using the INOVA 400MHz nuclear magnetic resonance instrument. The dispersion of m-MWCNTs was observed by TecnaiG220 transmission electron microscopy (TEM). The morphology of the fibers was examined using a Hitachi S–4700 field-emission scanning electron microscope (SEM) with an accelerating voltage of 15 kV after sputter coating the samples with platinum. Fourier transform infrared (FTIR) spectra of the fibers were recorded between 500 and 4000 cm^{-1} on a Thermo Scientific Nicolet iS10 infrared spectrometer. Differential scanning calorimetric (DSC) analysis was performed on TA Q200 equipment. The melting enthalpy (ΔH_m) and degree of crystallinity (X_c) were determined from the heating scan. Mechanical properties of the fibers were measured by an HD021N fiber strength instrument with gauge length 10 cm and a crosshead speed 20 mm min^{-1}, and the experimental results were evaluated as the averages of at least five measurements.

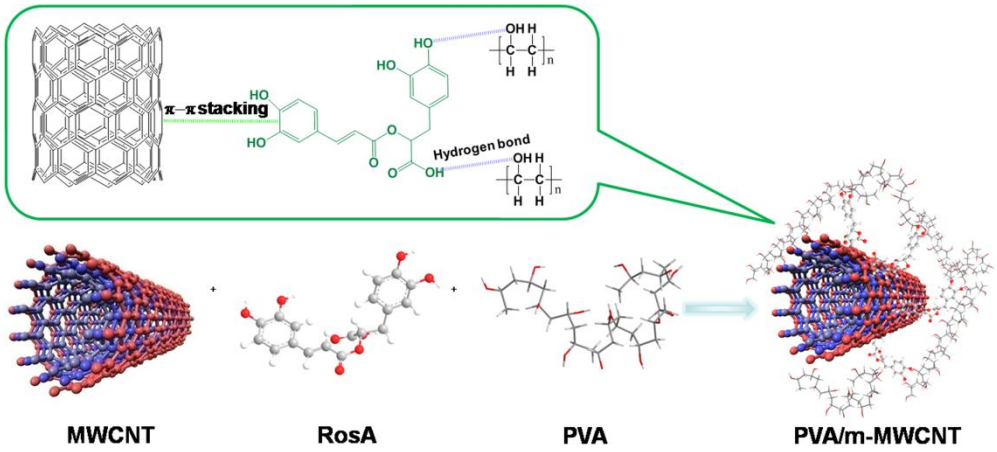

Fig. 2 Schematic illustration of the structure of PVA/m-MWCNTs composites.

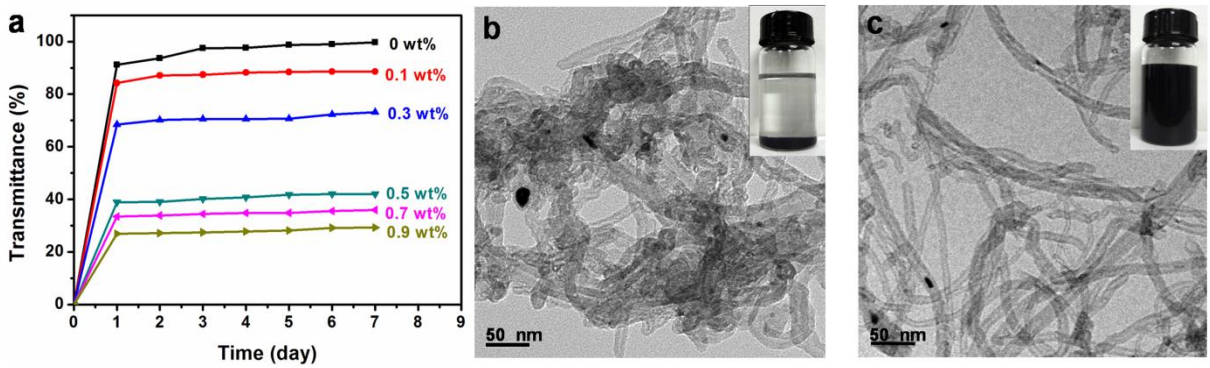

Fig. 3 UV−vis transmittances of the MWCNTs dispersions in DMSO/H_2O (vol ratio = 3/1) with different concentration of RosA marked on the ends of the curves (a) and TEM images of p-MWCNTs (b), m-MWCNTs (c) in DMSO/H_2O. The inserts are the corresponding MWCNTs dispersions after staying for 7 days.

3. Results and Discussion

According to schematic illustration as shown in Fig. 2, π-π stacking interaction exists between MWCNTs and RosA in the structure of m-MWCNTs, and hydrogen bonds are supposed to be formed between hydroxyl groups of RosA molecules on m-MWCNTs and PVA.

One of the effective ways to evaluate the dispersity of MWCNTs is measuring the stability of its suspension, which can be determined by measuring the UV transmittance of the supernatant, and generally higher MWCNTs concentration causes lower UV transmittance. p-MWCNTs and m-MWCNTs were dispersed into DMSO/H_2O mixed solvent (vol ratio=3/1) with stirring for 20 min and then left free-standing for different period of time. The transmittances at 259 nm as the characteristically absorption wavelength of MWCNTs at different standing time were measured.

As shown in Fig. 3a, p-MWCNTs (the upmost curve) exhibit almost 100% transmittances after staying one day, indicating poor dispersity in the solution, while this phenomenon changes for m-MWCNTs. As the concentration of RosA increases, the transmittance quickly decreases, particularly for RosA concentration 0.5wt%, proving good dispersity of m-MWCNTs. Because of the good dispersity at this concentration, the following m-MWCNTs mixed with PVA are all treated with 0.5wt% RosA loading.

Fig. 3b and 3c are TEM images of p-MWCNTs and m-MWCNTs in DMSO/H_2O (vol ratio = 3/1). Aggregation, entanglement and apparent piling up of p-MWCNTs DMSO/H_2O solvent are seen in Fig. 3b, while for m-MWCNTs, the tubes are obviously disentangled, separated and homogeneously distributed in the same solvent as shown in Fig. 3c. The inset picture provides much intuitive evidences for the dispersibility of p-MWCNTs and m-MWCNTs in the solvent. It is thought that the dispersion of MWCNTs is caused by π-π stacking of benzene rings on RosA with the graphitic lattice of the nanotubes as mentioned above. So it is understandable that m-MWCNTs can be dispersed in DMSO/H_2O through the bridge effect of RosA, leading to the disaggregation of m-MWCNTs bundles and providing a stable dispersion with the help of sonication and mechanical homogenization.

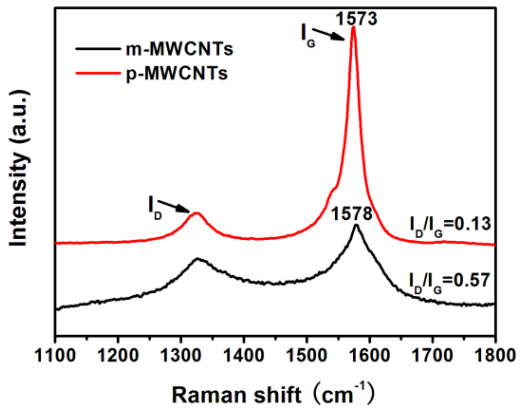

Fig. 4 Raman characterization of p-MWCNTs and m-MWCNTs.

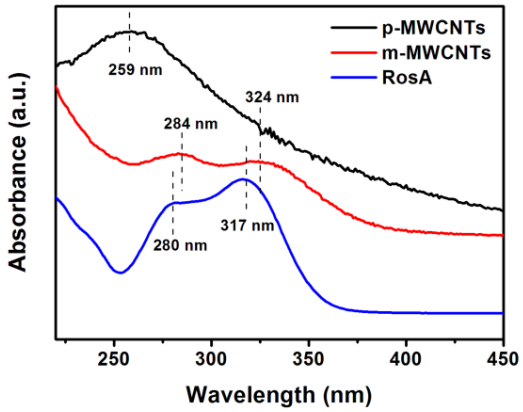

Fig. 5 UV–vis spectra of p-MWCNTs, m-MWCNTs and RosA.

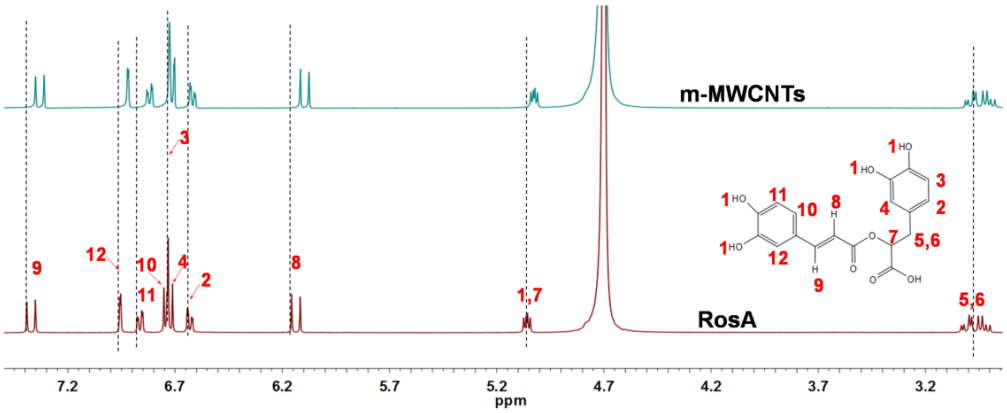

Fig. 6 ^{1}H NMR spectra of m-MWCNTs dispersion and RosA in D_2O.

Raman spectroscopy has historically been used to probe structural and electronic characteristics of graphite structure materials, providing useful information on the sp3 hybridized carbons or structural defect sites of the sp2 hybridized carbon network (D-band), in-plane vibration of sp2 carbon atoms (G-band) [31]. Consequently, the intensity ratio of the D and G bands (I_D/I_G) can be used to obtain information regarding structural changes of CNT [32]. Fig. 4 shows Raman spectra of the MWCNTs before and after modified with RosA. I_D/I_G of p-MWCNTs is about 0.13, while it increases to 0.57 for m-MWCNTs, which may well be attributed to π electron cloud staking between MWCNTs and the aromatic rings of RosA. Additionally, slight red-shifting to higher wavenumber (5 cm^{-1}) for G-band of m-MWCNTs than that of p-MWCNTs is also attributed to the strong π–π interaction between MWCNTs and RosA as reported by Kim [33].

UV–vis absorption spectra are recorded in Fig. 5. The absorption of RosA appears at 280 and 317 nm corresponding to the benzene ring and the double bond close to the benzene ring structure, and p-MWCNTs only have a characteristic peak at 259 nm. The absorption peak of p-MWCNTs disappears completely in m-MWCNTs since the mass fraction of RosA is far over that of p-MWCNTs, and the peaks of RosA red shift to 284 and 324 nm. According to molecular orbital theory, the electron around the benzene ring on RosA delocalized into the entire m-MWCNTs conjugated system, which leads to the reducing of the energy required for π-π transition, resulting in the absorption peak of m-MWCNTs red shifting. On the other hand, the benzene ring acts as an electron-donating group. When the benzene ring and m-MWCNTs form π-π conjugated system, the electron-donating group has higher reduction activity, causing lower energy to charge transfer transition and the absorption wavelength red shifting. Therefore the π-π stacking interaction between RosA and MWCNTs sidewalls is considered responsible for the absorption wavelength red shifting of RosA.

Fig. 6 shows the ^{1}H NMR spectra of m-MWCNTs and RosA in D_2O, which is used to demonstrate the stacking interaction between RosA and MWCNTs, and detect the accurate structure in the stacking system. In general, the electron cloud density around proton of RosA which is close to the surface of m-MWCNTs increases due to the conjugation effect. In other words, the diamagnetic shielding effect of m-MWCNTs will be more pronounced as the proton is closer to its surface, and the peaks will shift to upfield.

As shown in Fig. 6, the chemical shifts of peaks 2, 3, 4 belonging to one of the benzene rings almost do not change, illustrating that the corresponding benzene ring is not influenced by MWCNTs. However, peaks 8, 9, 10, 11, 12 belonging to the other ring all shift to upfield, suggesting that the benzene ring attaching the carbon carbon double bond has formed π-π stacking interaction with the MWCNTs. Although there are two benzene rings in RosA structure, only one of them can interact with MWCNTs due to the large steric hindrance. A similar phenomenon was observed and reported for other molecular modified carbon nanotubes through π-π stacking interaction [34].

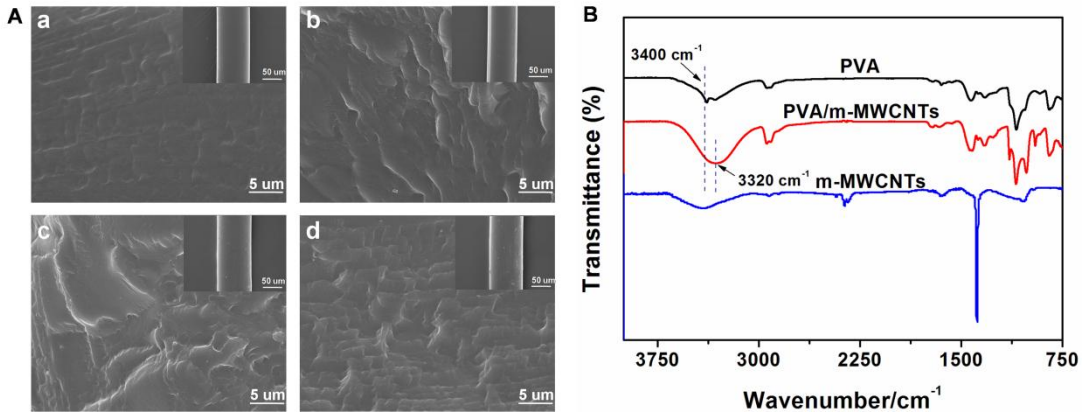

Fig. 7 (A) Selected SEM images of cross-sections and surfaces of PVA/m-MWCNTs composite fibers containing different amount of m-MWCNTs: (a) 0 wt%, (b) 0.2 wt%, (c) 0.6 wt%, (d) 1 wt%. (B) FTIR spectra of m-MWCNTs, neat PVA fiber and PVA/m-MWCNTs composite fiber containing 0.6 wt% m-MWCNTs.

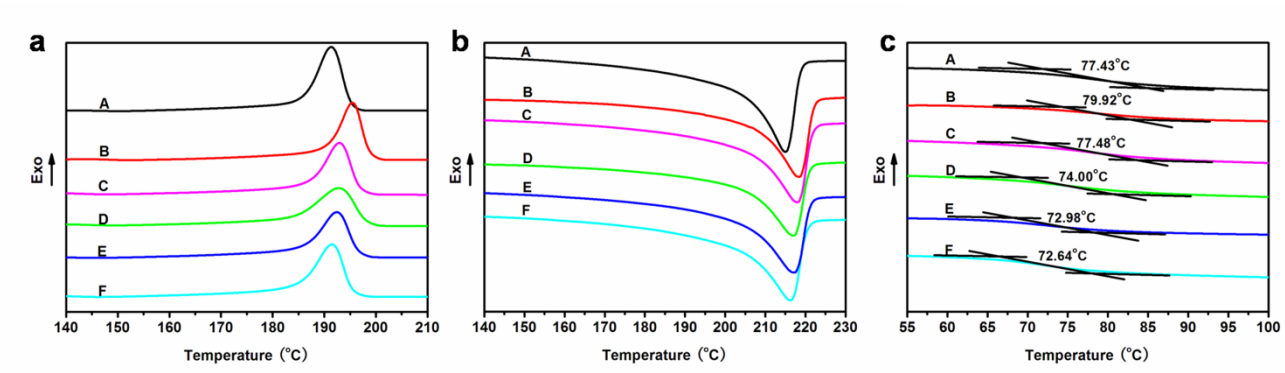

Fig. 8 DSC curves of PVA/m-MWCNTs composite fibers:(a) T_c, (b) T_m and (c)T_g with different m-MWCNTs contents: (A) 0 wt%, (B) 0.2 wt%, (C) 0.4wt%, (D) 0.6wt%, (E) 0.8 wt%, (F) 1 wt%.

Table 1 Thermal properties and crystallinity (X_c) of PVA/m-MWCNTs composite fibers.

MWCNTs content (wt %)	T_c (°C)	T_m (°C)	T_g (°C)	ΔH_m(J/g)	X_c (%)
0	191.36	215.07	77.43	50.44	36.39
0.2	195.43	218.58	79.92	46.03	33.21
0.4	193.00	217.91	77.48	47.37	34.18
0.6	192.90	217.16	74.00	43.25	31.20
0.8	192.45	217.11	72.98	49.88	35.99
1	191.46	216.28	72.64	46.76	33.74

Fig. 7A shows a typical SEM image of cross-sections and surfaces of PVA/m-MWCNTs composite fibers containing different amount of m-MWCNTs. As shown in Fig. 7A, the pure PVA fiber has a smooth cross section, but becomes gradually rough with increasing m-MWCNTs loading, which is considered to result from the gradually strengthening MWCNT-polymer interaction [35]. As shown in the inserts of Fig. 7A, except for pure PVA, the composite fiber with 0.2wt% m-MWCNTs loading also has a smooth and homogenous surface with almost no particles, indicating that m-MWCNTs are homogeneously dispersed in PVA without aggregation, and the surface of the composite fiber containing 0.6wt% m-MWCNTs is also smooth except some uniformly distributed small white dots, indicating that m-MWCNTs are homogeneously dispersed in PVA without aggregation. Small projections and bigger white particles begin to appear on the surfaces of the composite fibers containing 1wt% m-MWCNTs which is possibly because of the agglomeration of m-MWCNTs. Generally, better dispersion of m-MWCNTs means better reinforcing effect, resulting in higher strength of the composite fibers. Fig. 7B shows FTIR spectra of m-MWCNTs, neat PVA fiber and PVA/m-MWCNTs composite fiber containing 0.6 wt% m-MWCNTs. The peak at the vicinity of 3400 cm^{-1} is associated to typical stretching absorption of -OH, and it obviously band shifts to a lower frequency and widens for the composite fiber compared with neat PVA fiber and m-MWCNTs, which means that the nonbonded 'free' hydroxyls on PVA and RosA connected with MWCNTs have been engaged in hydrogen bonding between PVA and RosA on m-MWCNTs.

The DSC curves of PVA/m-MWCNTs composite fibers are shown in Fig. 8. The specimens were first heated from room temperature to 250 °C at a heating rate of 10 °C min^{-1} and kept for 10 min to erase the thermal history. The crystallization behaviors, i.e. cooling curves, were recorded from 250 to 40 °C at cooling rates of 10 °C min^{-1}. And then the specimens were second heated from 40 to 250 °C at a heating rate of 10 °C min^{-1} to obtain

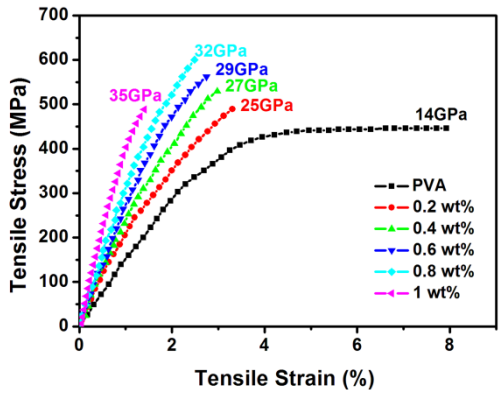

Fig. 9 Stress-strain curves of PVA/m-MWCNTs composite fibers with different m-MWCNTs loading, the values on the tips of curves are Young's modulus of the corresponding fibers.

heating curves. It can be seen from Fig. 8a that the incorporation of m-MWCNTs with PVA leads to increase in crystallization temperature (T_c) for the composites in comparison with that of neat PVA. But T_c decreases with increasing MWCNTs content, which is likely because too many dispersed MWCNTs act as nucleation agents during crystallization of PVA, leading to more imperfect crystals. Besides, adding more m-MWCNTs into PVA will disturb the regularity of PVA chains, resulting in decrease of crystallizability. On the other hand, m-MWCNTs and the strong interaction between m-MWCNTs and PVA matrix can also depress the crystal growth due to hindering the mobility of PVA chains.

As shown in Fig. 8b and Table 1, the melting temperature (T_m) of PVA/m-MWCNTs composites has similar trend to T_c, which is considered to be caused by the similar reasons. The glass transition temperatures (T_g) of the PVA/m-MWCNTs composite fibers first increase and then decrease as shown in Fig. 8c and Table 1. As mentioned above, H-bond interactions exist between the hydroxyl groups of RosA attached to the surface of m-MCWNTs and the same groups of the PVA chains. These H-bond interactions between PVA and m-MWCNTs and between PVA molecules are expected to affect the mobility of PVA polymer chains, causing the T_g of the composite fibers to be higher than that of pure PVA fibers. In addition, more MWCNTs can possibly hinder the formation of hydrogen bonds between PVA molecules, leading to decrease of T_g.

According to DSC data, X_c of the composite fibers is calculated as follows:

$$X_C = \frac{\Delta H_m}{w\Delta H_O}$$

where ΔH_m is measured from DSC and ΔH_0 is the enthalpy of pure PVA crystal (138.6 J g^{-1}).[36] As shown in Table 1, the X_c of PVA/m-MWCNTs composite fibers is somewhat lower than that of pure PVA fiber. It is deduced that the addition of the MWCNTs as a nucleating agent can change the nucleation and crystal growth mechanism of PVA.

Typical stress–strain curves and Young's modulus for the pure PVA fiber and PVA/m-MWCNTs composite fibers are shown in Fig. 9. The addition of small amounts of m-MWCNTs leads to a significant increase from 446 to 600 MPa for tensile strength with increasing the amount of m-MWCNTs loadings from 0 to 0.8 wt%, but as m-MWCNTs loading up to 1 wt%, the strength

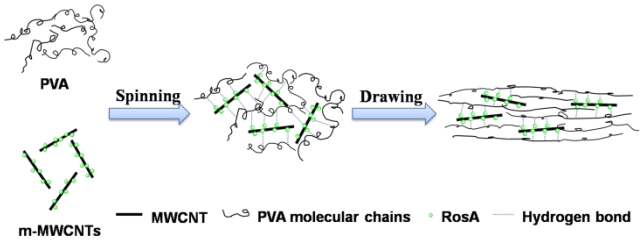

Fig. 10 Proposed structural model of the PVA/m-MWCNTs composites fibers.

decreases to 481 MPa instead, which suggests agglomerates of m-MWCNTs in the composite fibers. The Young's modulus (35 GPa) of the composite fibers containing 1 wt% m-MWCNTs loading is more than twice that of pure PVA fibers (14GPa). Compared with the pure PVA fiber, the maximum strain at fracture of the composite fibers decreases with the increasing of the m-MWCNTs content, possibly because the joint points between m-MWCNTs and PVA molecules of the composite fibers restrain the extension of the molecular chains when the composite fibers are drawn during the measurement. However, the composite fibers are still tough fibers with increased strength and modulus. The significant increases of the tensile strength and Young's modulus are suggested to be mainly due to the good dispersion of m-MWCNTs and the efficient stress transfer from the matrix to m-MWCNTs through interface bonding.[37] It has to point out that although the crystallinity decreases with the increase of m-MWCNTs loadings, it is considered that enforcing effect of m-MWCNTs to PVA and the interactions between PVA and m-MWCNTs dominate the increase of mechanical properties of the composite fibers.

The structural model of the PVA/m-MWCNTs composite fibers is shown in Fig. 10. In PVA/m-MWCNTs as-spun fibers, RosA adheres to MWCNTs by π-π stacking, while m-MWCNTs and PVA connects by H-bonding interactions between the hydroxyl groups of them. When the as-spun fibers are drawn, the molecular chains of the PVA matrix orient, resulting in strengthening their interfacial bonding, which leads to more load transferring from the PVA matrix to m-MWCNTs and higher fiber mechanical properties.

4. Conclusions

RosA is a green, non-toxic and much more environment-friendly natural phenolic compound. We found that RosA solution is a good selection as a modifier to functionalize MWCNT by π-π stacking, which is confirmed by Raman and ^{1}H NMR characterization. The mixture formed by mixing m-MWCNTs with PVA is obviously uniform compared with p-MWCNTs, and the homogeneous dispersion could stay stable for a long period of time in a DMSO/H_2O mixed solvent, which is caused by the interaction of hydrogen bonding between PVA and m-MWCNTs. The composite fibers of PVA/m-MWCNTs were prepared by wet-spinning the dispersion and drawing. And outstanding increments in tensile strength and Young's modulus of the PVA fibers were achieved due to enforcement of the nanotube and interaction between PVA and m-MWCNT for the composite fibers.

Notes and references

* *College of Chemistry, Chemical Engineering and Materials Science, Soochow University, Suzhou, Jiangsu, 215123, People's Republic of China. Fax: +86-0512-65880906; Tel: +86-0512-65880906 Email address: dailixing@suda.edu.cn*

1 M. F. De Volder, S. H. Tawfick, R. H. Baughman and A. J. Hart, *Science*, 2013, **339**, 535.
2 S. B. Sinnott and R. Andrews, *Crit. Rev. Solid State*, 2001, **26**, 145.
3 Y. Liu, Y. H. Choi, H. G. Chae, P. Gulgunje and S. Kumar, *Polymer*, 2013, **54**, 4003.
4 W. Li, S. Chou, J. Wang, H. Liu and S. Dou, *Nano Lett.*, 2013, **13**, 5480.
5 M. Moniruzzaman and K. I. Winey, *Macromolecules*, 2006, **39**, 5194.
6 X. Zhang, Q. Li, Y. Tu, Y. Li, J. Y. Coulter, L. Zheng, Y. Zhao, Q. Jia, D. E. Peterson and Y. Zhu, *Small*, 2007, **3**, 244.
7 N. Grossiord, J. Loos, O. Regev and C. E. Koning, *Chem. Mater.*, 2006, **18**, 1089.
8 N. Karousis, N. Tagmatarchis and D. Tasis, *Chem. Rev.*, 2010, **110**, 5366.
9 V. C. Moore, M. S. Strano, E. H. Haroz, R. H. Hauge, R. E. Smalley, J. Schmidt and Y. Talmon, *Nano Lett.*, 2003, **3**, 1379.
10 J. Liu, A. G. Rinzler, H. Dai, J. H. Hafner, R. K. Bradley, P. J. Boul, A. Lu, T. Iverson, K. Shelimov and C. B. Huffman, *Science*, 1998, **280**, 1253.
11 T. Saito, K. Matsushige and K. Tanaka, *Physica B: Condensed Matter*, 2002, **323**, 280.
12 Y. Lin, B. Zhou, K. Shiral Fernando, P. Liu, L. F. Allard and Y.-P. Sun, *Macromolecules*, 2003, **36**, 7199.
13 Y. Wang, Z. Iqbal and S. V. Malhotra, *Chem. Phys. Lett.*, 2005, **402**, 96.
14 P. Wang, C. N. Moorefield, S. Li, S.-H. Hwang, C. D. Shreiner and G. R. Newkome, *Chem. Commun.*, 2006, 1091.
15 Z. Yinghuai, A. T. Peng, K. Carpenter, J. A. Maguire, N. S. Hosmane and M. Takagaki, *J. Am. Chem. Soc.*, 2005, **127**, 9875.
16 S. J. Pastine, D. Okawa, B. Kessler, M. Rolandi, M. Llorente, A. Zettl and J. M. Fréchet, *J. Am. Chem. Soc.*, 2008, **130**, 4238.
17 J. J. Stephenson, J. L. Hudson, A. D. Leonard, B. K. Price and J. M. Tour, *Chem. Mater.*, 2007, **19**, 3491.
18 C. D. Doyle, J.-D. R. Rocha, R. B. Weisman and J. M. Tour, *J. Am. Chem. Soc.*, 2008, **130**, 6795.
19 K. Sadowska, K. Roberts, R. Wiser, J. Biernat, E. Jabłonowska and R. Bilewicz, *Carbon*, 2009, **47**, 1501.
20 D. Wunderlich, F. Hauke and A. Hirsch, *J. Mater. Chem.*, 2008, **18**, 1493.
21 T. S. Balaban, M. C. Balaban, S. Malik, F. Hennrich, R. Fischer, H. Rösner and M. M. Kappes, *Adv. Mater.*, 2006, **18**, 2763.
22 T. Fujigaya and N. Nakashima, *Polym. J.*, 2008, **40**, 577.
23 M. J. O'connell, S. M. Bachilo, C. B. Huffman, V. C. Moore, M. S. Strano, E. H. Haroz, K. L. Rialon, P. J. Boul, W. H. Noon and C. Kittrell, *Science*, 2002, **297**, 593.
24 M. Islam, E. Rojas, D. Bergey, A. Johnson and A. Yodh, *Nano Lett.*, 2003, **3**, 269.
25 E. A. Whitsitt and A. R. Barron, *Nano Lett.*, 2003, **3**, 775.
26 Y. Lin, L. F. Allard and Y.P. Sun, *The Journal of Physical Chemistry B*, 2004, **108**, 3760.
27 Y. Liu, J. Tang, X. Chen and J. Xin, *Carbon*, 2005, **43**, 3178.
28 G. Nakamura, K. Narimatsu, Y. Niidome and N. Nakashima, *Chem. Lett.*, 2007, **36**, 1140.
29 L. Lu, W. Hou, J. Sun, J. Wang, C. Qin and L. Dai, *J. Mater. Sci.*, 2014, **49**, 3322.
30 P. Zhang, D. Qiu, H. Chen, J. Sun, J. Wang, C. Qin and L. Dai, *Journal of Materials Chemistry A*, 2015, **3**, 1442.
31 M. Pimenta, G. Dresselhaus, M. S. Dresselhaus, L. Cancado, A. Jorio and R. Saito, *Phys. Chem. Chem. Phys.*, 2007, **9**, 1276.
32 K. A. Wepasnick, B. A. Smith, J. L. Bitter and D. Howard Fairbrother, *Anal Bioanal Chem*, 2010, **396**, 1003.
33 K. H. Kim and W. H. Jo, *Macromolecules*, 2007, **40**, 3708.
34 Q. Yang, L. Shuai and X. Pan, *Biomacromolecules*, 2008, **9**, 3422.
35 X. Zhang, X. Fan, H. Li and C. Yan, *J. Mater. Chem.*, 2012, **22**, 24081.
36 N. A. Peppas and E. W. Merrill, *J. Appl. Polym. Sci.*, 1976, **20**, 1457.
37 F. H. Gojny, M. H. Wichmann, B. Fiedler and K. Schulte, *Compos. Sci. Technol.*, 2005, **65**, 2300.

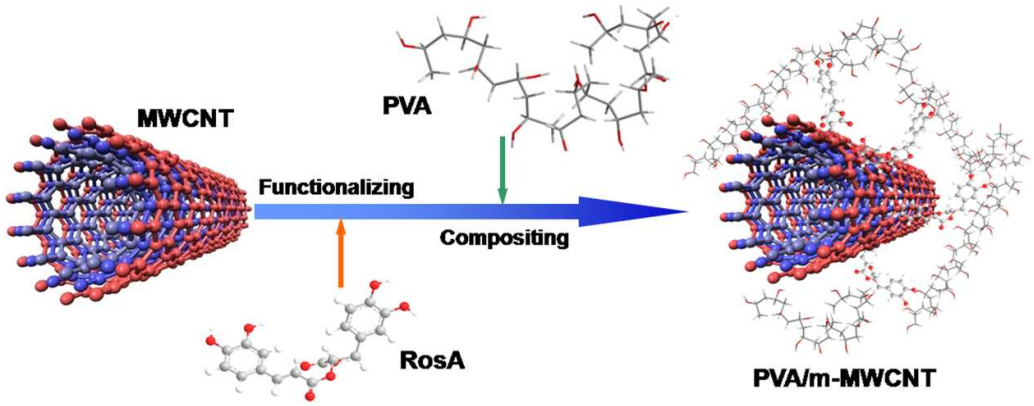

MWCNTs were functionalized with RosA through π–π stacking and then blended with PVA to form PVA/m-MWCNTs composite.